

# Aspects of gluon propagation in Landau gauge: spectral densities, and mass scales at finite temperature\*

PAULO J. SILVA, ORLANDO OLIVEIRA

Centro de Física Computacional, Universidade de Coimbra, Portugal  
DAVID DUDAL

KU Leuven Campus Kortrijk - KULAK, Department of Physics, Etienne  
Sabbelaan 53, 8500 Kortrijk, Belgium

Department of Physics and Astronomy, Ghent University, Belgium  
PEDRO BICUDO

CFTP, Instituto Superior Técnico, Portugal  
NUNO CARDOSO

NCSA, University of Illinois, Urbana IL 61801, USA

We discuss a method to extract the Källén-Lehmann spectral density of a particle (be it elementary or bound state) propagator and apply it to compute gluon spectral densities from lattice data. Furthermore, we also consider the interpretation of the Landau-gauge gluon propagator at finite temperature as a massive-type bosonic propagator.

PACS numbers: 11.10.Wx, 11.15.Ha, 12.38.Aw, 14.70.Dj

## 1. Spectral densities

In general, an Euclidean momentum-space propagator  $\mathcal{G}(p^2) \equiv \langle \mathcal{O}(p)\mathcal{O}(-p) \rangle$  of a (scalar) physical degree of freedom ought to have a Källén-Lehmann spectral representation

---

\* Presented at the “Workshop on Unquenched Hadron Spectroscopy: Non-Perturbative Models and Methods of QCD vs. Experiment”, at the occasion of Eef van Beveren’s 70th birthday, 1-5 September 2014, University of Coimbra, Portugal

$$\mathcal{G}(p^2) = \int_0^\infty d\mu \frac{\rho(\mu)}{p^2 + \mu}. \quad (1)$$

The knowledge of the spectral function  $\rho(\mu)$  is useful for, amongst other things, to get the masses of the physical states described by the operator  $\mathcal{O}$ .

Here we describe a method to compute the spectral density given a numerical estimate of the propagator, computed using e.g. lattice techniques. Note that eq. (1) is equivalent to a double Laplace transform  $\mathcal{G} = \mathcal{L}^2 \hat{\rho} = \mathcal{L} \mathcal{L}^* \hat{\rho}$  where  $(\mathcal{L}f)(t) \equiv \int_0^\infty ds e^{-st} f(s)$ ; the (double) inversion is then a notorious ill-posed problem, due to the exponential dampening.

For positive spectral functions, a popular approach is the maximum entropy method [1]. An alternative approach, aiming to compute spectral densities not necessarily positive, has been developed by some of us [2], based on the Tikhonov regularization supplemented with the Morozov discrepancy principle.

Specifically, setting  $D_i \equiv D(p_i^2)$  and assuming we have  $N$  data points, we minimize

$$\mathcal{J}_\lambda = \sum_{i=1}^N \left[ \int_{\mu_0}^{+\infty} d\mu \frac{\rho(\mu)}{p_i^2 + \mu} - D_i \right]^2 + \lambda \int_{\mu_0}^{+\infty} d\mu \rho^2(\mu) \quad (2)$$

where we use lattice data in momentum space for the gluon propagator computed in a  $80^4$  volume, with  $\beta = 6.0$  (Wilson gauge action) [3]. In eq. (2),  $\lambda > 0$  is a regularization parameter designed to overcome the ill-posed nature of the inversion. We choose  $\lambda$  by means of the Morozov principle: the optimal value  $\bar{\lambda}$  is such that the quality of the inversion is equal to the error on the data, i.e.  $\|D^{reconstructed} - D^{data}\| = \delta$  where  $\delta$  is the total noise on the input data. The IR regulator (threshold)  $\mu_0$  will be determined self-consistently by means of the optimal (Morozov) regulator  $\bar{\lambda}$ : we take the minimal value for  $\bar{\lambda}(\mu_0)$  that can be reached by varying  $\mu_0$ .

The minimization of (2) proceeds through a linear perturbation of  $\rho$  and imposing the vanishing of the variation of  $\mathcal{J}_\lambda$ ,

$$\sum_{i=1}^N \underbrace{\left[ \int_{\mu_0}^{+\infty} d\nu \frac{\rho(\nu)}{p_i^2 + \nu} - D_i \right]}_{\equiv c_i} \frac{1}{p_i^2 + \mu} + \lambda \rho(\mu) = 0 \quad (\mu \geq \mu_0) \quad (3)$$

The Källén-Lehmann inverse can be computed explicitly

$$\rho_\lambda(\mu) = -\frac{1}{\lambda} \sum_{i=1}^N \frac{c_i}{p_i^2 + \mu} \theta(\mu - \mu_0), \quad (4)$$

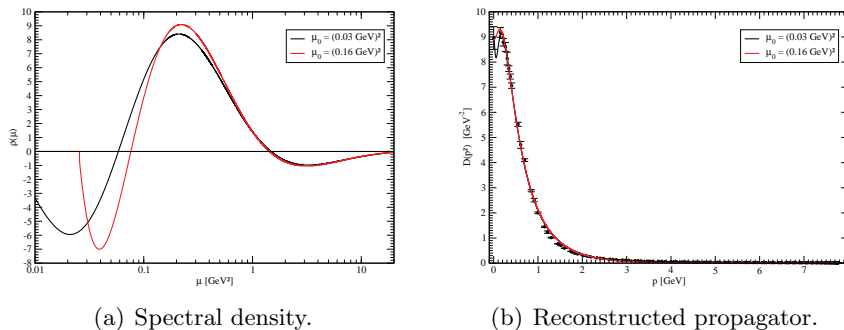


Figure 1. Results for the gluon spectral function and the reconstructed propagator vs. the input data. We refer to the main text and [2] for additional details.

where  $\theta(\cdot)$  is the Heaviside step function. We get a linear system for the coefficients  $c_i$ :

$$\lambda^{-1} \mathcal{M}c + c = -D \quad (5)$$

with

$$\mathcal{M}_{ij} = \int_{\mu_0}^{+\infty} d\nu \frac{1}{p_i^2 + \nu} \frac{1}{p_j^2 + \nu} = \frac{\ln \frac{p_j^2 + \mu_0}{p_i^2 + \mu_0}}{p_j^2 - p_i^2}. \quad (6)$$

In Figure 1 we plot the spectral density and, as a check, the reconstructed propagator which can be easily computed combining eqs. (4) and (1). In this case, we have two minima for  $\bar{\lambda}(\mu_0)$ , at  $\mu_0 \approx 0.03 \text{ GeV}^2$  and  $\mu_0 \approx 0.16 \text{ GeV}^2$ . We display the results for both values. We conclude that the gluon spectral density is indeed a nonpositive quantity. This is not surprising, since the gluons are not part of the physical spectrum [4]. In the near future, we plan to apply this method to glueballs<sup>1</sup> and other physical degrees of freedom.

## 2. Gluon mass at finite temperature

In this section we briefly describe a recent investigation by some of us [6], where we address the interpretation of the Landau gauge gluon propagator at finite temperature as a massive-type bosonic propagator. For such a goal, we consider a Yukawa-type propagator

$$D(p) = \frac{Z}{p^2 + m^2}, \quad (7)$$

where  $m$  is the gluon mass and  $Z^{\frac{1}{2}}$  the overlap between the gluon state and the quasi-particle massive state.

<sup>1</sup> See [5] for a preliminary study of glueball spectral densities.

Temp. (MeV)	$\beta$	$L_s$	$L_t$	$a$ (fm)	$1/a$ (GeV)
121	6.0000	64	16	0.1016	1.9426
162	6.0000	64	12	0.1016	1.9426
194	6.0000	64	10	0.1016	1.9426
243	6.0000	64	8	0.1016	1.9426
260	6.0347	68	8	0.09502	2.0767
265	5.8876	52	6	0.1243	1.5881
275	6.0684	72	8	0.08974	2.1989
285	5.9266	56	6	0.1154	1.7103
290	6.1009	76	8	0.08502	2.3211
305	6.1326	80	8	0.08077	2.4432
324	6.0000	64	6	0.1016	1.9426
366	6.0684	72	6	0.08974	2.1989
397	5.8876	52	4	0.1243	1.5881
428	5.9266	56	4	0.1154	1.7103
458	5.9640	60	4	0.1077	1.8324
486	6.0000	64	4	0.1016	1.9426

Table 1. Lattice setup used for the computation of the gluon propagator at finite temperature. Simulations used the Wilson gauge action;  $\beta$  was adjusted to have a constant physical volume,  $L_s a \simeq 6.5$  fm. For the generation of gauge configurations and Landau gauge fixing, we used Chroma [7] and PFFT [8] libraries.

At finite temperature, the Landau gauge gluon propagator is splitted into two components

$$D_{\mu\nu}^{ab}(\hat{q}) = \delta^{ab} \left( P_{\mu\nu}^T D_T(q_4, \vec{q}) + P_{\mu\nu}^L D_L(q_4, \vec{q}) \right) \quad (8)$$

where  $D_T$  and  $D_L$  are the transverse and longitudinal propagators respectively.

The lattice setup for the simulations at finite temperature considered here is described in Table 1. The surface plots of the two form factors can be seen in Figure 2. For further details see [6].

A simple definition for a mass scale associated with the gluon propagator can be given by

$$m = 1/\sqrt{D(p^2 = 0; T)} . \quad (9)$$

Our results for such a mass scale are shown in Figure 3.

A more realistic value for the gluon mass can be obtained by a fit to the lattice data in the infrared region using the ansatz described in eq. (7). It turns out that the transverse form factor is not described by a Yukawa-type

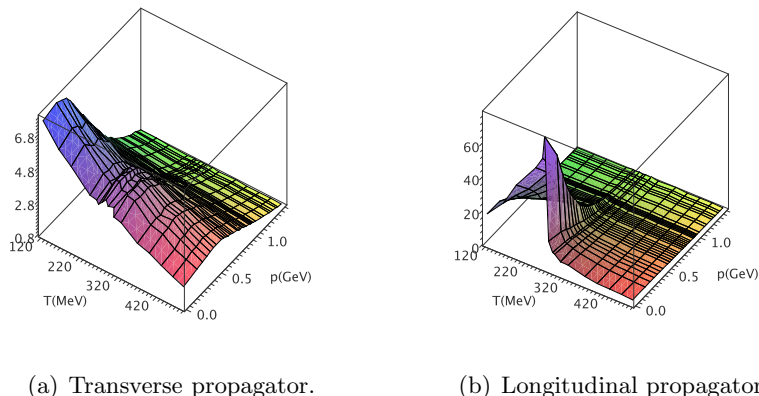


Figure 2. Components of the gluon propagator as a function of momentum and temperature.

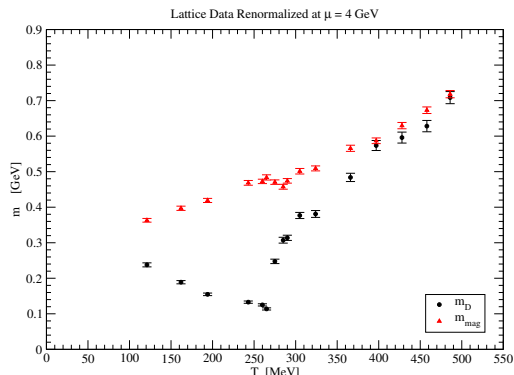


Figure 3. Electric and magnetic mass defined from zero momentum propagators.

propagator. Therefore one concludes that  $D_T$  does not behave as quasi-particle massive boson for  $T < 500$  MeV. In what concerns the longitudinal form factor, we report the values of  $Z(T)$  and  $m_g(T)$  in Figure 4.

We observe that both  $m_g(T)$  and  $Z(T)$  are sensitive to the confinement-deconfinement phase transition; the data suggests that the phase transition is of first order. Below  $T_c$ , the gluon mass is a decreasing function of  $T$ , whereas it increases for  $T > T_c$ . Furthermore, the gluon mass follows the expected perturbative behaviour for  $T > 400$  MeV.

### Acknowledgments

Work supported by FCT via projects PTDC/FIS/100968/2008, CERN/FP/123612/2011, and CERN/FP/123620/2011 developed under the initia-

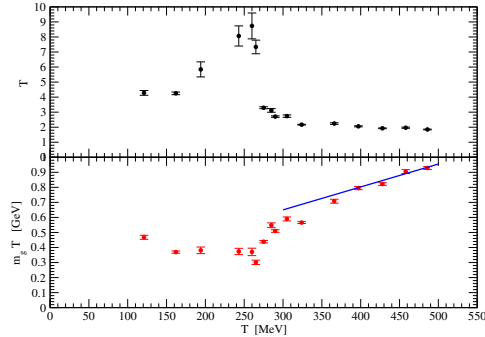


Figure 4.  $Z(T)$  and  $m_g(T)$  from fitting the longitudinal gluon propagator to a Yukawa form. The curve in the lower plot is the fit of  $m_g$  to the functional form predicted by perturbation theory.

tive QREN financed by the UE/FEDER through the Programme COMPETE - Programa Operacional Factores de Competitividade. P. J. Silva supported by FCT grant SFRH/BPD/40998/2007. D. Dudal acknowledges financial support from the Research-Foundation Flanders (FWO Vlaanderen) via the Odysseus grant of F. Verstraete. Nuno Cardoso supported by NSF award PHY-1212270.

## References

- [1] M. Asakawa, T. Hatsuda and Y. Nakahara, Prog. Part. Nucl. Phys. **46** (2001) 459.
- [2] D. Dudal, O. Oliveira and P. J. Silva, Phys.Rev. D **89** (2014) 014010, arXiv:1310.4069 [hep-lat].
- [3] O. Oliveira and P. J. Silva, Phys. Rev. D **86** (2012) 114513, arXiv:1207.3029 [hep-lat].
- [4] J. M. Cornwall, Mod. Phys. Lett. A **28** (2013) 1330035, arXiv:1310.7897 [hep-ph].
- [5] O. Oliveira, D. Dudal, P. J. Silva, PoS(Lattice 2012)214, arXiv:1210.7794 [hep-lat].
- [6] P. J. Silva, O. Oliveira, P. Bicudo and N. Cardoso, Phys.Rev. D **89** (2014) 074503, arXiv:1310.5629 [hep-lat].
- [7] R. G. Edwards and B. Joó, Nucl.Phys.Proc.Suppl. **140** (2005) 832, arXiv:hep-lat/0409003.
- [8] M. Pippig, SIAM J. Sci. Comput. **35**, C213 (2013).